

Synthesis and Characterization of $[\text{NH}_2\text{C}(\text{I})=\text{NH}_2]_3\text{MI}_5$ (M = Sn, Pb): Stereochemical Activity in Divalent Tin and Lead Halides Containing Single $\langle 110 \rangle$ Perovskite Sheets

Shumin Wang,[†] David B. Mitzi,* Chris A. Feild, and Arnold Guloy[‡]

Contribution from the IBM T. J. Watson Research Center, P.O. Box 218, Yorktown Heights, New York 10598, and Department of Chemistry and Texas Center for Superconductivity, University of Houston, Houston, Texas 77204-5641

Received December 28, 1994[⊗]

Abstract: Isotopic crystals with the composition $[\text{NH}_2\text{C}(\text{I})=\text{NH}_2]_3\text{MI}_5$ (M = Sn, Pb) were grown from an aqueous solution. The compounds crystallize in the monoclinic space group $P2_1/c$ with an unusual layered organic–inorganic structural type. The structure is configured in a manner that iodoformamidinium cation layers terminate the three-dimensional cubic perovskite structure along the $[110]$ direction, resulting in single $\langle 110 \rangle$ -oriented $[\text{NH}_2\text{C}(\text{I})=\text{NH}_2]\text{MI}_3$ (M = Sn, Pb) perovskite sheets, which are actually characterized by infinite, corner-sharing, one-dimensional MI_5 octahedral chains held together by iodoformamidinium cations. The structural formula can be expressed as $[\text{NH}_2\text{C}(\text{I})=\text{NH}_2]_2[\text{NH}_2\text{C}(\text{I})=\text{NH}_2]\text{MI}_5$, which is closely related to the recently discovered series of $\langle 110 \rangle$ -oriented layered perovskites, $[\text{NH}_2\text{C}(\text{I})=\text{NH}_2]_2(\text{CH}_3\text{NH}_3)_m\text{Sn}_m\text{I}_{3m+2}$. A close comparison of the title compounds with the $\langle 110 \rangle$ series is carried out. The distorted tin/lead iodine octahedral geometries observed in the title compounds indicate that the lone pair electrons of tin(II) and lead(II) are stereochemically active, with the lone pair effect being stronger in the tin compound. The progressive evolution of the lone pair stereoactivity as well as the transitions of structural dimensionality and transport properties of these $\langle 110 \rangle$ -oriented compounds will be discussed.

Introduction

Recently much attention has been devoted to organic–inorganic multilayered perovskites due to the tuneability of their special structural features and interesting physical properties. These compounds are involved in various fundamental as well as more applied studies related to their transport^{1,2} optical,^{3–5} thermochromic,⁶ or structural^{7–9} properties. Their structures are characterized by slabs of multilayer perovskite sheets alternating with organic, such as alkylammonium, cation layers. The physical and structural properties of these compounds can be fine tuned by substituting or tailoring the organic cation layer.

A family of conducting layered organic–inorganic perovskites, $(\text{C}_4\text{H}_9\text{NH}_3)_2(\text{CH}_3\text{NH}_3)_{n-1}\text{Sn}_n\text{I}_{3n+1}$ ($n = 1–5$), noted as the $\langle 100 \rangle$ series, has been reported¹ not long ago, in which the inorganic slabs, containing “ n ” $\langle 100 \rangle$ -terminated $\text{CH}_3\text{NH}_3\text{SnI}_3$ perovskite sheets, alternate with butylammonium bilayers. These conducting non-oxide layered perovskites share many of the structural features of the cuprate superconductors. Following

the discovery of the $\langle 100 \rangle$ series, another unusual class of conducting layered halides, $[\text{NH}_2\text{C}(\text{I})=\text{NH}_2]_2(\text{CH}_3\text{NH}_3)_m\text{Sn}_m\text{I}_{3m+2}$, was identified.² This series appears to be stabilized by the interposed layers of iodoformamidinium cations terminating the basic cubic perovskite structure on the $\langle 110 \rangle$ crystallographic plane, rather than the $\langle 100 \rangle$ plane, forming slabs of “ m ” $\langle 110 \rangle$ -oriented $\text{CH}_3\text{NH}_3\text{SnI}_3$ perovskite sheets. The formation of these two halide families has shown the ability to stabilize an organic-based layered perovskite structure with either $\langle 100 \rangle$ - or $\langle 110 \rangle$ -oriented sheets through the use of different organic cations, namely butylammonium or iodoformamidinium cations. It therefore demonstrates that the flexibility provided by the organic cation layer extends beyond simply changing spacing between inorganic perovskite sheets (through choice of organic cation length) to a more direct influence on the inorganic perovskite sheets themselves, i.e., the orientation of the perovskite sheets.² Furthermore, a semiconductor–metal transition with increasing “ n ” and “ m ” was observed in the $\langle 100 \rangle$ and $\langle 110 \rangle$ families.^{1,2} This provides a suitable model for experimental and theoretical studies of the behavior of delocalized electrons with respect to the structural low-dimensionality, as well as the structure–property correlation, and it may help provide an understanding of unusual physical phenomena, such as high-temperature superconductivity, observed in low-dimensional solids.

While higher members ($m \geq 2$) have been reported² in the $\langle 110 \rangle$ series, $[\text{NH}_2\text{C}(\text{I})=\text{NH}_2]_2(\text{CH}_3\text{NH}_3)_m\text{Sn}_m\text{I}_{3m+2}$, there has been no evidence of the $m = 1$ member thus far. Further investigation of the $m = 1$ phase is interesting not only to extend the series of structures but, more importantly, because the structural building unit changes from two-dimensional $\langle 110 \rangle$ -oriented perovskite sheets to one-dimensional chains of corner sharing octahedra in going from the higher “ m ” to the $m = 1$ structures. It will be interesting to understand how the compound formation is affected by this and what it takes to stabilize the $m = 1$ structure.

* Author to whom correspondence should be addressed at the IBM T. J. Watson Research Center.

[†] Permanent address: University of Houston.

[‡] University of Houston.

[⊗] Abstract published in *Advance ACS Abstracts*, May 1, 1995.

(1) Mitzi, D. B.; Feild, C. A.; Harrison, W. T. A.; Guloy, A. M. *Nature* **1994**, *369*, 467.

(2) Mitzi, D. B.; Wang, S.; Feild, C. A.; Chess, C. A.; Guloy, A. M. *Science* **1995**, *267*, 1473.

(3) Ishihara, T.; Takahashi, J.; Goto, T. *Phys. Rev. B* **1990**, *42*, 11099.

(4) Calabrese, J.; Jones, N. L.; Harlow, R. L.; Thorn, D.; Wang, Y. *J. Am. Chem. Soc.* **1991**, *113*, 2328.

(5) Papavassiliou, G. C.; Koutselas, I. B.; Terzis, A.; Whangbo, M.-H. *Solid State Commun.* **1994**, *91*, 695.

(6) Mostafa, M. F.; Abdel-Kader, M. M.; Arafat, S. S.; Kandeel, E. M. *Phys. Scr.* **1991**, *43*, 627.

(7) Arend, H.; Tichy, K.; Baberschke, K.; Rys, F. *Solid State Commun.* **1976**, *18*, 999.

(8) Tieke, B.; Chapuis, G. *Mol. Cryst. Liq. Cryst.* **1986**, *137*, 101.

(9) Needham, G. F.; Willett, R. D.; Franzen, H. F. *J. Phys. Chem.* **1984**, *88*, 674.

In the present article, we report the formation of new low-dimensional organic-inorganic halides, $[\text{NH}_2\text{C}(\text{I})=\text{NH}_2]_3\text{MI}_5$ ($\text{M} = \text{Sn}, \text{Pb}$). These compounds are closely related to the $[\text{NH}_2\text{C}(\text{I})=\text{NH}_2]_2(\text{CH}_3\text{NH}_2)_m\text{Sn}_m\text{I}_{3m+2}$ series. In fact, they can be considered as the first member ($m = 1$) of this series with, however, the substitution of $[\text{NH}_2\text{C}(\text{I})=\text{NH}_2]^+$ for CH_3NH_3^+ on the "A" site of the perovskite slab. The synthesis and the structure are described, and a comparison of the title compounds with the related (110) series is carried out. In $[\text{NH}_2\text{C}(\text{I})=\text{NH}_2]_3\text{MI}_5$ ($\text{M} = \text{Sn}, \text{Pb}$), the tin/lead atoms sit in irregular iodine octahedral environments suggesting that their non-bonding lone pair electrons are stereochemically active. The Sn(II) lone pair is more active compared to that of Pb(II) as observed by the larger distortion for the SnI_6 octahedra. In addition, the stereochemical activity is found to be more important in the title tin compound than in the more conducting higher members ($m \geq 2$) of the related (110) series.

Experimental Section

Synthesis. Crystals of the title compounds in this study were grown from a slowly cooled concentrated aqueous hydriodic acid solution in an argon atmosphere to prevent oxidation. For the tin-containing system, a total charge of 0.5 g of NH_2CN (0.126 g, 3.0 mmol) and SnI_2 (0.374 g, 1 mmol) were dissolved in 10 mL of 57 wt % aqueous HI solution at 80 °C. The solution was cooled from 80 to -10 °C at 2 °C/h. The crystalline products were filtered under nitrogen from which column-like orange crystals were obtained. The products were dried in flowing argon at 80 °C for several hours and then removed to an argon-filled drybox with oxygen and water levels maintained below 1 ppm. The product was shown to contain a significant amount of iodoformamidinium iodide transparent crystals, as characterized by X-ray powder diffraction. The crystals of the title compounds can be easily separated due to the distinct color and morphology. Crystals of the lead analogue were grown in a similar way, except for starting with a 1:1:1 molar ratio of $\text{CH}_3\text{NH}_2 \cdot \text{HI}$ (0.480 g, 3.02 mmol), NH_2CN (0.127 g, 3.02 mmol), and PbI_2 (1.393 g, 3.02 mmol). The reactants were dissolved in 17 mL of 57 wt % aqueous hydriodic acid at 60 °C. The solution was soaked at 60 °C for 24 h before being cooled to -10 °C at 2 °C/h. After dwelling at -10 °C for 10 h the crystals were filtered from the solution and dried. Yellow transparent crystals were obtained in ca. 95% yield with a minor secondary phase which was characterized to be the $m = 2$ lead analogue of the (110) series.

In the synthesis of the title compounds, cyanamide is used as a starting material for the formation of the iodoformamidinium cation. Anhydrous addition reaction between nitriles and hydrogen halides generally results in imidyl halides which are usually basic enough to accept a proton to form a salt.¹⁰ In aqueous acid solutions, however, cyanamide most commonly hydrolyzes to give urea. Kilpatrick¹¹ has demonstrated that the rate of hydrolysis of cyanamide in aqueous nitric acid solutions increases continuously with increasing acid concentration. For hydrochloric and hydrobromic acids, the rate increases to a maximum with increasing acid concentration and thereafter drops off as a result of the formation of competing less hydrolyzable species. It is likely that our use of the stronger concentrated aqueous hydriodic acid effectively avoids the hydrolysis of cyanamide through a similar process, with the formation of the more hydrolysis-resistant iodoformamidinium cation found in these new materials.

X-ray Crystallography. Suitable single crystals were selected under a microscope (inside the drybox) and sealed in quartz capillaries. One of the difficulties encountered in this crystallographic study is the severe absorption due to the heavy atoms such as Sn, Pb, and I. The size and shape of the crystals are crucial. Relatively small and cylindrical crystals (approximate dimensions $0.05 \times 0.05 \times 0.5$ mm) were chosen to generate reasonably intense reflections without excessive absorption. Data for the title compounds were collected at room temperature on an Enraf-Nonius CAD4 diffractometer with graphite monochromatized Mo K α radiation. The data collection parameters and the structural

Table 1. Parameters of Data Collection and Structure Refinement for $[\text{NH}_2\text{C}(\text{I})=\text{NH}_2]_3\text{MI}_5$ ($\text{M} = \text{Sn}, \text{Pb}$)

formula	$[\text{NH}_2\text{C}(\text{I})=\text{NH}_2]_3\text{SnI}_5$	$[\text{NH}_2\text{C}(\text{I})=\text{NH}_2]_3\text{PbI}_5$
formula weight	1266.076	1354.576
crystal color	orange	yellow
crystal system	monoclinic	monoclinic
space group	$P2_1/c$	$P2_1/c$
a , Å	6.4394(4)	6.4240(5)
b , Å	20.069(2)	20.087(2)
c , Å	18.722(1)	18.752(2)
β , deg	92.822(6)	92.906(8)
V , Å ³	2416.5(3)	2416.7(4)
Z	4	4
ρ_{calcd} , g/cm ³	3.480	3.723
radiation (λ), Å	Mo K α (0.7093)	Mo K α (0.7093)
absorption coeff (μ), cm ⁻¹	43.2	171.6
transmission	0.7825–1.0000	0.6195–1.0000
factor range		
scan mode	$\omega-2\theta$	$\omega-2\theta$
2θ range, deg	$5.2 \leq 2\theta \leq 56.0$	$5.0 \leq 2\theta \leq 50.0$
data collected	$\pm h, k, l$	$\pm h, k, l$
R_{int}	0.011	0.131
no. of data collected	7574	4384
no. of unique data	7008	4249
no. of data used in refinement	3799 ($I > 3\sigma(I)$)	2313 ($I > 3\sigma(I)$)
no. of variables	118	118
R_F^a	0.049	0.060
R_w^b	0.052	0.069

$$^a R_F = \sum(F_o - F_c) / \sum(F_o). \quad ^b R_w = \{\sum w(F_o - F_c)^2 / \sum (wF_o^2)\}^{1/2}.$$

refinement results are tabulated in Table 1. The unit cell parameters and the crystal orientation matrix were obtained by least-squares fit of 25 reflections with $20^\circ < 2\theta < 53^\circ$ for tin and $12^\circ < 2\theta < 29^\circ$ for lead compounds, respectively. Intensity control reflections were monitored every 5000 s during the data collection. Significant degradation (approximately 34% and 14% drops in the intensity control reflections for the tin and lead compounds, respectively) was observed during data collection and accounted for during data analysis. The NRCVAX 386 PC version¹² program was used for the structural solution and refinement. The space group $P2_1/c$ was chosen for both compounds based on systematic observations of $h0l$, $l = 2n$; $0k0$, $k = 2n$; $00l$, $l = 2n$ and the successful structural refinements. The intensity data were corrected for Lorentz and polarization effects. Empirical absorption corrections based on several azimuthal scans were also applied. The positions of tin and lead atoms were determined from Patterson maps. The remaining non-hydrogen atomic positions were picked up from the Fourier difference maps. Locating the hydrogen atoms was not attempted. All the heavy tin/lead and iodine atoms were refined anisotropically, while the light nitrogen and carbon atoms were refined isotropically. The atomic positions and isotropic thermal parameters of the tin and lead compounds are tabulated in Tables 2 and 3, respectively. The anisotropic temperature factors for both title compounds are supplied as supplementary material (Tables S.I and S.II).

Results and Discussions

Structural Description. Both tin and lead compounds crystallize in a monoclinic crystal system with the same structure type. Single crystal structural studies yield the compositional formula $[\text{NH}_2\text{C}(\text{I})=\text{NH}_2]_3\text{MI}_5$ ($\text{M} = \text{Sn}, \text{Pb}$). Figure 1 shows the ORTEP drawing of a half unit cell of $[\text{NH}_2\text{C}(\text{I})=\text{NH}_2]_3\text{SnI}_5$ along the b -axis. In this structure, each tin atom is connected to six iodine atoms at distances ranging from 2.957 to 3.484 Å forming a distorted octahedron (detailed bond distances and angles are shown in Tables 4 and 5). This distortion is presumably caused by the stereochemical activity of the tin(II) lone pair electrons, which will be discussed in

(10) Zil'berman, E. N. *Russian Chem. Rev.* **1962**, *31*, 615.

(11) Kilpatrick, M. L. *J. Am. Chem. Soc.* **1947**, *69*, 40.

(12) Gabe, E. J.; Le Page, Y.; Charland, J.-P.; Lee, F. L.; White, P. S. *J. Appl. Crystallogr.* **1989**, *22*, 384.

(13) Lide, D. R. *Tetrahedron* **1962**, *17*, 125.

Table 2. Positional and Thermal Parameters^a for $[\text{NH}_2\text{C}(\text{I})=\text{NH}_2]_3\text{SnI}_5$

atom	position	x	y	z	B_{iso} (\AA^2)
Sn	4e	0.9466(2)	0.12952(5)	0.24747(6)	3.05(4)
I(1)	4e	0.4060(2)	0.12646(6)	0.24980(8)	4.64(6)
I(2)	4e	0.9104(2)	0.23824(6)	0.12916(6)	4.12(5)
I(3)	4e	0.9290(2)	0.01836(6)	0.13259(6)	3.88(5)
I(4)	4e	0.9537(2)	0.02142(6)	0.37805(6)	3.68(4)
I(5)	4e	0.9734(2)	0.26007(7)	0.35465(6)	4.34(5)
I(6)	4e	0.6436(2)	0.42734(6)	0.20313(9)	5.66(7)
I(7)	4e	0.2930(2)	0.32254(6)	0.04195(6)	4.13(5)
I(8)	4e	0.5894(2)	0.14925(8)	-0.05748(7)	5.04(6)
C(1)	4e	0.411(3)	0.3616(8)	0.2356(9)	3.4(3)
N(1)	4e	0.221(3)	0.3816(9)	0.243(1)	5.7(4)
N(2)	4e	0.465(3)	0.2982(8)	0.2461(9)	4.8(3)
C(2)	4e	0.522(3)	0.372(1)	-0.015(1)	4.4(3)
N(3)	4e	0.718(3)	0.357(1)	0.000(1)	7.4(5)
N(4)	4e	0.455(3)	0.423(1)	-0.059(1)	7.2(5)
C(3)	4e	0.363(3)	0.1125(9)	0.0090(9)	3.7(3)
N(5)	4e	0.172(2)	0.1289(8)	-0.0035(8)	4.3(3)
N(6)	4e	0.430(3)	0.069(1)	0.062(1)	6.5(4)

^a Heavy atoms (Sn and I) are refined anisotropically. Anisotropic thermal parameters are found in supplementary Table S.I.

Table 3. Positional and Thermal Parameters^a for $[\text{NH}_2\text{C}(\text{I})=\text{NH}_2]_3\text{PbI}_5$

atom	position	x	y	z	B_{iso} (\AA^2)
Pb	4e	0.9422(2)	0.12871(7)	0.24782(9)	3.85(6)
I(1)	4e	0.4378(4)	0.1258(1)	0.2506(2)	5.4(1)
I(2)	4e	0.9105(4)	0.2406(1)	0.1292(2)	4.7(1)
I(3)	4e	0.9328(4)	0.0171(1)	0.1295(2)	4.4(1)
I(4)	4e	0.9542(4)	0.0206(1)	0.3778(1)	4.1(1)
I(5)	4e	0.9755(4)	0.2577(1)	0.3557(2)	4.9(1)
I(6)	4e	0.6435(5)	0.4270(1)	0.2050(2)	6.4(2)
I(7)	4e	0.2938(4)	0.3245(1)	0.0429(2)	4.7(1)
I(8)	4e	0.5907(4)	0.1516(2)	-0.0569(2)	5.4(1)
C(1)	4e	0.414(6)	0.362(2)	0.239(2)	4.1(7)
N(1)	4e	0.231(5)	0.383(2)	0.248(2)	5.5(8)
N(2)	4e	0.462(5)	0.300(2)	0.244(2)	5.4(7)
C(2)	4e	0.515(6)	0.376(2)	-0.013(2)	4.1(7)
N(3)	4e	0.707(6)	0.362(2)	0.001(2)	6.7(9)
N(4)	4e	0.455(7)	0.421(2)	-0.059(2)	8.0(11)
C(3)	4e	0.370(6)	0.112(2)	0.009(2)	4.2(8)
N(5)	4e	0.177(5)	0.132(2)	-0.001(2)	4.8(7)
N(6)	4e	0.437(6)	0.071(2)	0.061(2)	7.0(10)

^a Heavy atoms (Pb and I) are refined anisotropically. Anisotropic thermal parameters are found in supplementary Table S.II.

detail later. The octahedra share opposite corners forming a one-dimensional SnI_5 octahedral chain extending along the [100] direction. The $\text{Sn}-\text{I}(1)-\text{Sn}$ angle of $177.30(5)^\circ$ indicates that the octahedral chain is close to being linear along the a -axis. Neighboring chains are held together by iodoformamidinium cations, $[\text{NH}_2\text{C}(\text{I})=\text{NH}_2]^+$.

There are three independent iodoformamidinium cation sites, noted as i(6), i(7), and i(8), corresponding to the labels of their iodine atoms for simplicity. Cations i(7) and i(8) are arranged in such a way that each of them forms an infinite "chain" along the a -axis. The resulting i(7) and i(8) "chains" are oriented "anti" to each other along the [010] direction forming iodoformamidinium cation layers parallel to the (001) plane. The SnI_5 octahedral chains are "sandwiched" by these organic layers (Figure 2). Furthermore, two edges provided by the octahedra from the neighboring SnI_5 chains, together with I(7) and I(8), from the i(7) and i(8) cations, delimit an irregular hexagonal channel (outlined in Figure 2) where the iodoformamidinium cation, i(6), is located. The refined iodine-carbon distances, 2.11(2), 2.12(2), and 2.09(2) \AA for i(6), i(7), and i(8), respectively, are similar to interatomic distances observed in other organic iodides. The refined bond angles (Table 5) around the carbons, ranging from $117(1)^\circ$ to $126(2)^\circ$, are consistent with

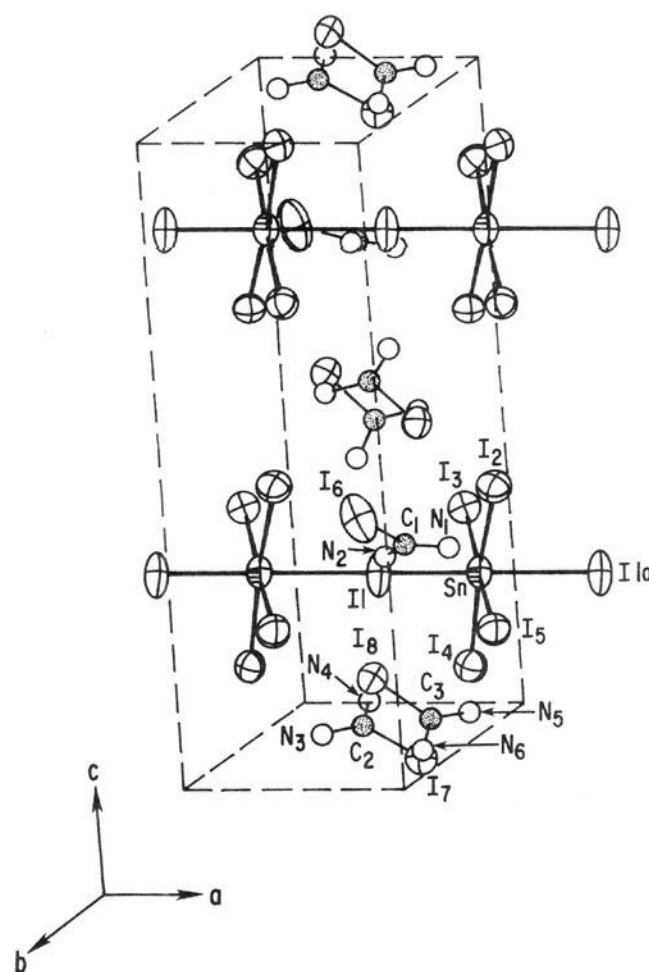


Figure 1. A half unit cell of $[\text{NH}_2\text{C}(\text{I})=\text{NH}_2]_3\text{SnI}_5$ along the b -axis, with the unit cell outlined, showing the detailed structure and the SnI_5 chains along the a -axis. The carbon atoms are shaded. The ellipsoids for tin and iodine atoms are drawn at 50% probability, while carbon and nitrogen sphere sizes are arbitrary.

Table 4. Selected Bond Distances in $[\text{NH}_2\text{C}(\text{I})=\text{NH}_2]_3\text{MI}_5$ (M = Sn, Pb)

atoms	distances (\AA)		atoms	distances (\AA)	
	M = Sn	M = Pb		M = Sn	M = Pb
M-I(1)	2.957(1)	3.182(3)	C(1)-N(1)	1.30(2)	1.27(5)
M-I(1) ^a	3.484(1)	3.243(3)	C(1)-N(2)	1.33(2)	1.28(5)
M-I(2)	3.110(2)	3.161(3)	C(2)-N(3)	1.32(3)	1.27(6)
M-I(3)	3.097(2)	3.153(3)	C(2)-N(4)	1.36(3)	1.30(6)
M-I(4)	3.267(2)	3.263(3)	C(3)-N(5)	1.28(2)	1.31(5)
M-I(5)	3.300(2)	3.287(3)	C(3)-N(6)	1.38(3)	1.32(6)
I(6)-C(1)	2.11(2)	2.10(4)	I(8)-C(3)	2.09(2)	2.09(4)
I(7)-C(2)	2.12(2)	2.08(4)			

^a $1 + x, y, z$.

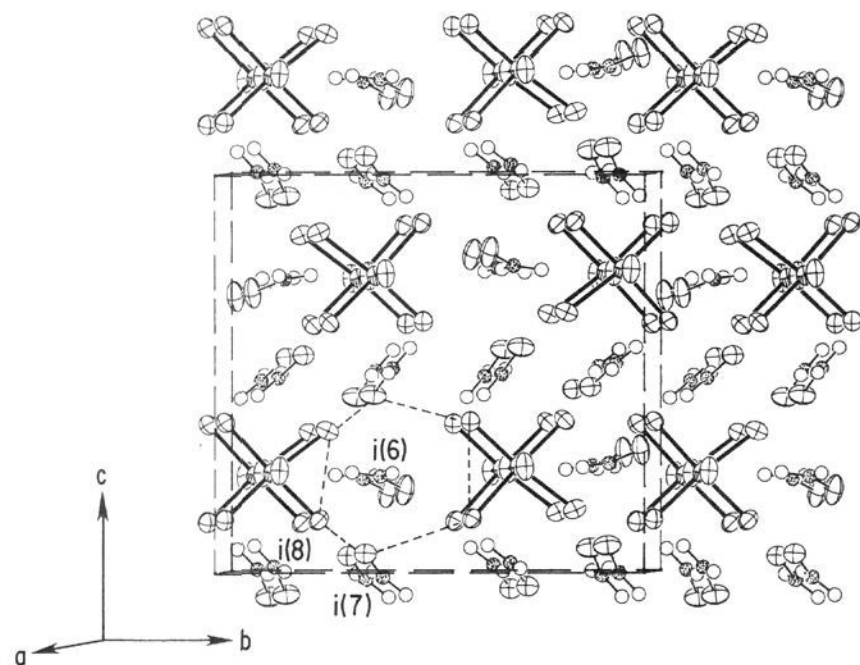
sp^2 orbital hybridization. The similarity between the two bond distances of carbon to nitrogen (Table 4) inside each iodoformamidinium cation suggests that the cations may have resonance structures, i.e. $[\text{NH}_2\text{C}(\text{I})=\text{NH}_2]^+$ vs $[\text{H}_2\text{N}=\text{C}(\text{I})\text{NH}_2]^+$.

$[\text{NH}_2\text{C}(\text{I})=\text{NH}_2]_3\text{PbI}_5$ is isostructural with $[\text{NH}_2\text{C}(\text{I})=\text{NH}_2]_3\text{SnI}_5$. The comparison of the bond distances and angles between these two compounds is tabulated in Tables 4 and 5. In comparison to the tin compound, a smaller "a" lattice parameter, 6.4240(5) versus 6.4394(4) \AA (for the tin compound), was observed for the lead analogue, despite the bigger size of the lead atom. This results from a stronger stereochemical activity of the tin(II) lone pair electrons indicated by the bigger distortion of the SnI_6 octahedra compared to PbI_6 (according to the M-I distances in Table 4).

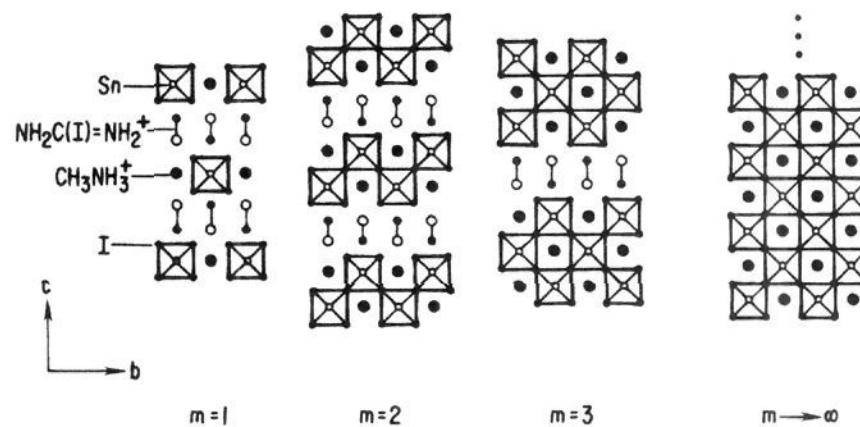
Structural Comparison to the $[\text{NH}_2\text{C}(\text{I})=\text{NH}_2]_2(\text{CH}_3\text{NH}_3)_m\text{Sn}_m\text{I}_{3m+2}$ Series. The structure of $[\text{NH}_2\text{C}(\text{I})=\text{NH}_2]_3\text{MI}_5$ (M = Sn, Pb) is closely related to that of $[\text{NH}_2\text{C}(\text{I})=\text{NH}_2]_2(\text{CH}_3\text{NH}_3)_m\text{Sn}_m\text{I}_{3m+2}$ (the $\langle 110 \rangle$ series). Figure 3 is a schematic drawing of the structure of the $\langle 110 \rangle$ series, of which the detailed structure of the $m = 2$ phase was reported.² The structure of this series consists of "m" layer thick perovskite slabs terminating on $\langle 110 \rangle$ surfaces of the three-dimensional $\text{CH}_3\text{NH}_3\text{SnI}_3$

Table 5. Selected Bond Angles in $[\text{NH}_2\text{C}(\text{I})=\text{NH}_2]_3\text{MI}_5$ ($\text{M} = \text{Sn}, \text{Pb}$)

atoms	angles (deg)	
	M = Sn	M = Pb
I(1)–M–I(1) ^a	177.30(5)	177.24(9)
I(1)–M–I(2)	93.73(4)	93.03(8)
I(1)–M–I(3)	89.87(4)	88.97(8)
I(1)–M–I(4)	89.89(4)	89.43(8)
I(1)–M–I(5)	89.15(4)	88.30(8)
I(1) ^a –M–I(2)	88.93(4)	89.72(8)
I(1) ^a –M–I(3)	89.62(4)	90.86(8)
I(1) ^a –M–I(4)	87.48(4)	87.83(8)
I(1) ^a –M–I(5)	91.65(4)	92.19(8)
I(2)–M–I(3)	90.68(4)	90.70(8)
I(2)–M–I(4)	175.32(5)	175.64(8)
I(2)–M–I(5)	82.87(4)	82.67(8)
I(3)–M–I(4)	92.30(4)	92.94(7)
I(3)–M–I(5)	173.40(5)	172.69(9)
I(4)–M–I(5)	94.23(4)	93.81(8)
M ^a –I(1)–M	177.30(5)	177.2(1)
I(6)–C(1)–N(1)	122(1)	120(3)
I(6)–C(1)–N(2)	117(1)	117(3)
N(1)–C(1)–N(2)	121(2)	122(4)
I(7)–C(2)–N(3)	117(2)	117(3)
I(7)–C(2)–N(4)	117(1)	119(3)
N(3)–C(2)–N(4)	126(2)	122(4)
I(8)–C(3)–N(5)	119(1)	117(3)
I(8)–C(3)–N(6)	117(1)	117(3)
N(5)–C(3)–N(6)	124(2)	124(4)

^a 1 + x, y, z.**Figure 2.** The extended structure of $[\text{NH}_2\text{C}(\text{I})=\text{NH}_2]_3\text{SnI}_5$ viewed along the a -axis, showing the structural arrangements of the tin iodine octahedral chains as well as the iodoformamidinium cations, i(6), i(7), and i(8). The unit cell is outlined by the long dashed lines, while the irregular hexagonal channel for i(6) is outlined by the short dashed lines. The carbon atoms are shaded. The ellipsoids for tin and iodine atoms are drawn at 50% probability, while carbon and nitrogen sphere sizes are arbitrary.

perovskite structure. This three-dimensional structure termination is accomplished by the insertion of iodoformamidinium cation layers, in which the cations are anti-parallel to each other along the b -axis. Lattice parameters for the observed members of $[\text{NH}_2\text{C}(\text{I})=\text{NH}_2]_2(\text{CH}_3\text{NH}_3)_m\text{Sn}_m\text{I}_{3m+2}$ approximately follow the rule, $a = a_p$, $b = \sqrt{2}a_p$, $c = K + ma_p/\sqrt{2}$, where a_p is defined as the lattice parameter for the cubic perovskite (for $\text{CH}_3\text{NH}_3\text{SnI}_3$, $a_p = 6.240 \text{ \AA}$), and $K \approx 5.95(5) \text{ \AA}$ is the thickness of the organic cation layer. Comparing Figure 2 and the $m = 1$ proposed structure in Figure 3 reveals their structural resemblance. They both contain single $\langle 110 \rangle$ -oriented perovskite sheets alternating with iodoformamidinium cation layers. How-

**Figure 3.** Schematic representation of the proposed structures of the $m = 1, 2, 3$, and ∞ (cubic perovskite) members of the $[\text{NH}_2\text{C}(\text{I})=\text{NH}_2]_2(\text{CH}_3\text{NH}_3)_m\text{Sn}_m\text{I}_{3m+2}$ series. The detailed structure of the $m = 2$ phase was reported elsewhere.²

ever, the “A” site cation, CH_3NH_3^+ in the ABX_3 perovskite slab, is substituted by the iodoformamidinium cation $[\text{NH}_2\text{C}(\text{I})=\text{NH}_2]^+$, i(6), in Figure 2. Therefore, the structural formula of Figure 2 can be written as $[\text{NH}_2\text{C}(\text{I})=\text{NH}_2]_2[\text{NH}_2\text{C}(\text{I})=\text{NH}_2]\text{SnI}_5$ in the notation of the $[\text{NH}_2\text{C}(\text{I})=\text{NH}_2]_2(\text{CH}_3\text{NH}_3)_m\text{Sn}_m\text{I}_{3m+2}$ series (with $m = 1$).

In contrast to the higher ($m \geq 2$) members of the $\langle 110 \rangle$ series, characterized by two-dimensional perovskite slabs, the structure of the title compound contains one-dimensional octahedral chains as building units. Presumably these chains are more flexible, therefore leaving more room in the “A” site for the bigger iodoformamidinium cation. In the structural transition from the higher members ($m \geq 2$) to the $m = 1$ phase, the structure along the a -axis stays approximately the same, so that $a = 6.4394(4) \text{ \AA} \approx a_p$. The lengthening of the “ a ” lattice parameter, 6.4394(4) versus 6.2726(3) \AA ($m = 2$), is at least partially the result of the stronger repulsion between the tin(II) lone pair electrons and the iodine anions. Switching from two-dimensionality to one-dimensionality of the building units releases all the atoms from the symmetry restricted positions (mirror plane and inversion center in $m = 2$ phase, for example) to the general positions in $[\text{NH}_2\text{C}(\text{I})=\text{NH}_2]_2[\text{NH}_2\text{C}(\text{I})=\text{NH}_2]\text{SnI}_5$, and consequently causes a doubling of the unit cell along both the c -axis (18.722(1) \AA) and the b -axis (20.069(2) \AA). The increase by 1.35 \AA ($b = 8.6878(5) \text{ \AA}$ in the $m = 2$ phase) along the b -axis is caused by the substitution of CH_3NH_3^+ by the more bulky iodoformamidinium cation. In the actual structure of this newly formed tin compound, the observed thickness of the iodoformamidinium layer, 4.81 \AA , is significantly smaller than K (5.95 \AA), perhaps because of the tilting of the cation layer, as seen in Figure 2.

It is important to point out that in the synthesis of the title compounds, attempts were made to form $[\text{NH}_2\text{C}(\text{I})=\text{NH}_2]_2(\text{CH}_3\text{NH}_3)\text{SnI}_5$, by incorporation of $\text{CH}_3\text{NH}_2 \cdot \text{HI}$ into the starting solution. Details of the synthesis of the corresponding Pb(II) samples, with $\text{CH}_3\text{NH}_2 \cdot \text{HI}$ in the starting solution, are given in the Experimental Section of this paper. Surprisingly, even in these runs, the $m = 1$ phase was only formed with the much larger cation $[\text{NH}_2\text{C}(\text{I})=\text{NH}_2]^+$, instead of CH_3NH_3^+ . This can be rationalized considering the fundamental difference between the structures of the $m = 1$ and higher members, i.e. one-dimensional octahedral chains versus two-dimensional $\text{CH}_3\text{NH}_3\text{SnI}_3$ perovskite sheets as structural building units. The environments for the “A” site cation are different in these two structures. In addition to the bigger size, $[\text{NH}_2\text{C}(\text{I})=\text{NH}_2]^+$ presents a very different geometry compare to $(\text{CH}_3\text{NH}_3)^+$, which may be preferred by the chain type arrangement.

The structure of the title compounds is also related to that of CaCrF_5 ¹⁴ and $(\text{NH}_4)_2\text{MnF}_5$ ¹⁵ in that they all contain one-dimensional corner sharing octahedral chains. In CaCrF_5 ,

however, the layer corresponding to the iodoformamidinium layer of the title compounds is missing. In contrast, the "A" cation in $(\text{NH}_4)_2\text{MnF}_5$ is absent, causing NH_4^+ in the cation layer to be displaced toward the "A" sites.

Stereochemical Activity of Sn(II) and Pb(II) Lone Pair Electrons. In $[\text{NH}_2\text{C}(\text{I})=\text{NH}_2]_3\text{MI}_5$ ($\text{M} = \text{Sn}, \text{Pb}$) compounds, the formal oxidation state of tin and lead is 2+, with $5s^2$ and $6s^2$ non-bonding lone pair electrons. The presence of the lone pairs generally results in a non-spherical charge distribution around tin/lead cations in solids, and furthermore, to a lowering of the symmetry of coordination of negative ions around them, so called being stereochemically active. The commonly observed coordinations of tin(II) and lead(II) cations are trigonal and square-pyramidal arrangements. A number of theoretical approaches have been used to explain the distorting effects of the non-bonding lone pair electrons,¹⁶⁻¹⁸ among which Brown's theory provides an adequate description of the use of the tin/lead valence electrons in bonding in the solid state.¹⁸ Brown's model assumes that the coordination polyhedron of the main group ns^2 elements is based on an octahedron which has been distorted so that the coordination of the lone pair cation can form a continuous series from one having 2 strong, 2 intermediate, and 2 weak bonds (a), through one having 3 strong and 3 weak bonds (b), to one having 1 strong, 1 weak, and 4 intermediate bonds (c). This model allows various intermediate configurations resulting from a progressive evolution of the lone pair activity, according to the strength of the bonds forming the octahedron. The commonly observed trigonal and square-pyramidal geometries are the extremes of (b) and (a) where the stereoactivity is maximum, since the lone pairs occupy the anion positions and can be regarded as ligands. In $[\text{NH}_2\text{C}(\text{I})=\text{NH}_2]_3\text{SnI}_5$, the irregular SnI_6 octahedron has the shortest bond (2.957 Å) and longest bond (3.484 Å) opposite to each other. A similar range of Sn-I bond distances of 2.94, 3.20, 3.23, 3.47, and 3.47 (in Å) was observed in monoclinic CsSnI_3 .¹⁹ The octahedral distortion in the title tin compound is an intermediate between (b) and (c) according to the Sn-I bond distances shown in Figure 4a. In Figure 4a, six Sn-I distances can be approximately segregated into two groups, {I(1), I(2), I(3)} and {I(1a), I(4), I(5)}, based on the Sn-I bond distances. The three iodines inside each group are related by a pseudo-3-fold axis. The lone pair of the tin(II) is probably oriented along this pseudo-3-fold axis in the direction of the {I(1a), I(4), I(5)} group, more toward the longest Sn-I(1a) bond, where the most room is available for the lone pair. In the lead compound, the geometry of PbI_6 adopts the distortion type (b), i.e. 3 strong and 3 weak bonds according to the observed Pb-I distances (shown in Figure 4b). This type of distorted octahedral coordination for lead(II) was also reported in $\text{Pb}_5\text{Ge}_3\text{O}_{11}$.²⁰

In general, the stereochemical activity of the lone pair is more important for small cations than for the bigger ones, i.e. it increases going up a column from the bottom of the periodic table, in agreement with the evolution of the covalent character of the elements. Therefore it is expected that the $5s^2$ lone pair of tin(II) is stereochemically more active than the $6s^2$ lone pair of lead(II). This is confirmed by comparing the Sn-I and Pb-I

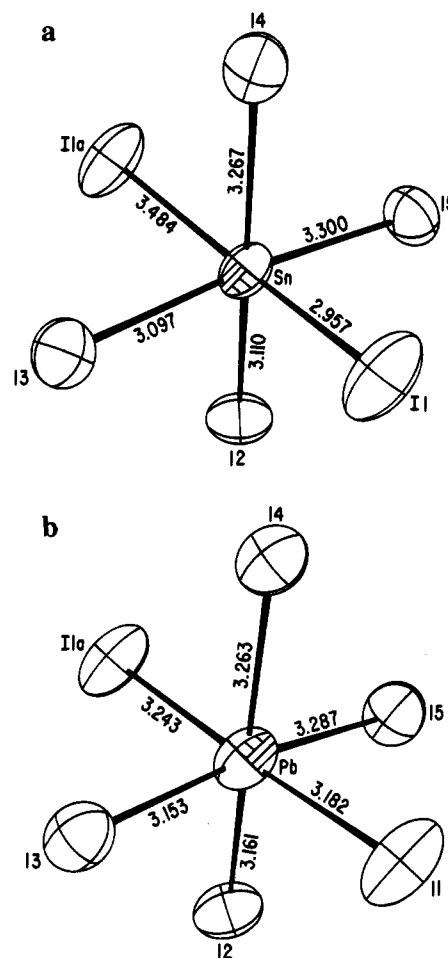


Figure 4. The ORTEP drawing of (a) SnI_6 and (b) PbI_6 octahedra showing the distortions indicated by the (Sn,Pb)-I bond distances.

distances (Table 4) and by examining the lattice constants of the title compounds (Table 1). The tin compound has an abnormally longer "a" lattice parameter, 6.4394(4) Å, compared to 6.4240(5) Å in the lead analogue, which is against what would be expected from Vegard's law. This is because the "a" lattice parameter of $[\text{NH}_2\text{C}(\text{I})=\text{NH}_2]_3\text{MI}_5$ ($\text{M} = \text{Sn}, \text{Pb}$) is basically determined by the sum of the apical M-I(1) and M-I(1a) lengths, as shown in Figure 1. In the tin compound, the most distortion occurs along the I(1)-Sn-I(1a) chain, i.e. the a-axis, resulting in an unusually long (3.484 Å) Sn-I bond which is not found in the lead analogue. Presumably this is attributed to the stronger repulsion of the tin(II) lone pair. In the meantime, the four basal Sn-I bonds in the octahedron associated with the bc-plane are more regular, therefore leading to the smaller "b" and "c" lattice parameters compared to the lead analogue as expected by Vegard's law. The lengthening of the "a" lattice parameter in the tin compound compensates for the size difference between tin and lead, resulting in approximately the same cell volume for both compounds, despite the larger size for lead than for tin.

From the above observations, it is fair to say that the lone pairs in both title compounds are stereochemically active. Both tin and lead cations are in low-symmetry environments. However, the repulsion from the lone pair on the anions is mild since there is still basically a 6-fold coordination around the tin and lead cations. Therefore, most likely the lone pair electrons are only partially localized in $5s^2$ and $6s^2$ orbitals of the tin(II) and lead(II) cations. In $[\text{NH}_2\text{C}(\text{I})=\text{NH}_2]_2(\text{CH}_3\text{NH}_3)_2\text{Sn}_2\text{I}_8$, the tin(II) atoms sit on a mirror plane in a slightly distorted octahedral geometry with the Sn-I bonds of 3.094(2), 3.094-

(14) (a) Dumora, D.; Von der Muhll, R.; Ravez, J. *Mat. Res. Bull.* **1971**, *6*, 561. (b) Wu, K. K.; Brown, I. D. *Mat. Res. Bull.* **1973**, *8*, 593.

(15) Sears, D. R.; Hoard, J. L. *J. Chem. Phys.* **1969**, *50*, 1066.

(16) Gillespie, R. J.; Nyholm, R. S. *Q. Rev. Chem. Soc.* **1957**, *11*, 339.

(17) Andersson, S.; Astrom, A. *NBS Special Publication, Solid State Chemistry; Proceedings of the 5th Materials Research Symposium*, No. 364, July 1972.

(18) Brown, D. J. *Solid State Chem.* **1974**, *11*, 214.

(19) Mauersberger, P.; Huber, F. *Acta Crystallogr.* **1980**, *B36*, 683.

(20) Kay, M. I.; Newnham, R. E.; Wolfe, R. W. *Ferroelectrics* **1975**, *9*, 1.

(2), 3.096(3), 3.179(3), 3.185(1), and 3.185(1) Å, which indicates a very weak but non-zero stereoactivity. In going to higher symmetry in the cubic $\text{CH}_3\text{NH}_3\text{SnI}_3$,²¹ the tin atoms sit in a perfect octahedral environment with the lone pair electrons being totally inactive. Presumably the distorting effect of the non-bonding electrons is reduced or removed by their populating an empty low-lying energy band in the solid.²² This so-called solid state effect generally gives rise to optical coloration and electrical conductivity. The title compounds present very light colors (Table 1). They are probably semiconductors with a large band gap. Meanwhile, $[\text{NH}_2\text{C}(\text{I})=\text{NH}_2]_2(\text{CH}_3\text{NH}_3)_2\text{Sn}_2\text{I}_8$ is a semiconductor² with a band gap of 0.33 eV which crystallizes in a dark color. Finally $\text{CH}_3\text{NH}_3\text{SnI}_3$ is a metal with a black appearance.²³

Conclusion

The low-temperature aqueous solution growth method has proven to be very useful in the crystal growth of the layered tin and lead organic-inorganic solid state materials. It overcomes the difficulty encountered in high-temperature solid state reactions due to the low thermal stability of these compounds. The formation of the layered $\langle 100 \rangle$ -oriented and $\langle 110 \rangle$ -oriented conducting perovskite halides, as well as the newly reported title compounds, has demonstrated the potential of the unusual organic-inorganic structural framework for their tuneability with respect to a given desired structure as well as physical properties. The report of the newly formed $[\text{NH}_2\text{C}(\text{I})=\text{NH}_2]_3\text{-MI}_5$ ($\text{M} = \text{Sn}, \text{Pb}$) compounds extends the $\langle 110 \rangle$ series, $[\text{NH}_2\text{C}(\text{I})=\text{NH}_2]_2(\text{CH}_3\text{NH}_3)_m\text{Sn}_m\text{I}_{3m+2}$, to include the end-member $m = 1$ compound. Iodoformamidinium cations play an important role in stabilizing the structure. More importantly, the observed structural transition from the distinct one-

(21) Weber, D. Z. *Naturforsch.* **1978**, *33b*, 862.

(22) Donaldson, J. D.; Grimes, S. M. *Rev. Silicon, Germanium, Tin, Lead Compd.* **1984**, *8*, 1.

(23) Mitzi, D. B.; Feild, C. A.; Schlesinger, Z.; Laibowitz, R. B. *J. Solid State Chem.* **1995**, *114*, 159.

dimensional chain of the title compounds, through the two-dimensional layer of the higher ($m \geq 2$) members, to the three-dimensional cubic perovskite structure of the end member demonstrates the richness of the compound formation and the structural spectrum provided by this family of materials. The compound formation and the structural knowledge carried out in this study lead to a further understanding of the $\langle 110 \rangle$ series. The reported semiconductor-metal transition² in these families provides a great opportunity for the systematic study of structure-property correlation in a conducting system.

Finally, the chemistry of tin and lead is in itself interesting. The lone pair electrons are found to be stereochemically active in the title compounds. The stereoactivity is reduced by the solid state effect in progressing toward the more conducting higher members of the studied series and eliminated in the metallic end member, the cubic perovskite, $\text{CH}_3\text{NH}_3\text{SnI}_3$. The study of the tin(II)/lead(II) lone pair stereochemical activity enriches our understanding of the chemistry of ns^2 main group elements in extended solid state lattices. From the fact that both tin and lead elements adopt the same structure type in the reported title compounds, it is expected that the lead analogues of the higher members in the $\langle 110 \rangle$ series form as well, and further studies are underway on these materials.

Acknowledgment. We thank B. A. Scott and A. J. Jacobson for stimulating discussions. One of us (S. Wang) also thanks the Texas Center for Superconductivity for financial support.

Supplementary Material Available: Tables showing anisotropic temperature factors for both the tin and lead compounds (1 page). This material is contained in many libraries on microfiche, immediately follows this article in the microfilm version of the journal, can be ordered from the ACS, and can be downloaded from the Internet; see any current masthead page for ordering information and Internet access instructions.

JA944181E